Virchows Archiv (2023) 482:567–580
https://doi.org/10.1007/s00428-022-03457-7

ORIGINAL ARTICLE

Uterine inflammatory myofibroblastic tumor harboring novel *NUDCD3-ROS1* and *NRP2-ALK* fusions: clinicopathologic features of 4 cases and literature review

Lili Zhang[1] · Lijuan Luan[1] · Licheng Shen[1] · Ruqun Xue[1] · Jie Huang[1] · Jieakesu Su[1] · Yufeng Huang[1] · Yifan Xu[1] · Xiang Wang[1] · Yang Shao[2,3] · Yuan Ji[1] · Chen Xu[1] · Yingyong Hou[1]

Received: 5 June 2022 / Revised: 2 November 2022 / Accepted: 14 November 2022 / Published online: 10 January 2023

Abstract

Inflammatory myofibroblastic tumor (IMT) is a mesenchymal neoplasm of intermediate biologic potential, which occurs mostly in the lung and abdomen cavity of children and young adults. Uterine IMTs are rare. Herein, we presented clinicopathologic features of 4 uterine IMTs. All four patients were initially diagnosed as leiomyosarcoma by other hospitals and corrected to uterine IMT after pathological consultation. Patient age ranged from 44 to 64 years old. Two cases demonstrated multiple masses. Microscopically, three tumors were composed of fascicular spindled cells with eosinophilic cytoplasm, and the other one was densely composed of spindled and epithelioid cells with bizarre and multinucleated cells. Tumor cells showed variable nuclear atypia, ranging from mild to severe. Prominent inflammatory cell infiltration was found in one case, and necrosis in two tumors. Immunochemistry staining revealed expression of smooth muscle markers in all four tumors, including a-SMA and desmin. Three tumors were positive for ALK protein expression. FISH analysis demonstrated *ROS1* rearrangement in one tumor and *ALK* rearrangement in the other 3 tumors. NGS analysis showed novel *NUDCD3-ROS1* and *NRP2-ALK* fusions in two tumors and *TNS1-ALK* fusion in the other two tumors. Gene aberrations involving p53 signaling pathway were identified in all four cases. All patients received surgery as primary treatment, and one had neoadjuvant chemotherapy. Three patients recurred within 12 months, and the other one recurred after 7 years. Patients with recurrence were treated with a combination of chemotherapy, targeted therapy, or surgery. In conclusion, the diagnosis of uterine IMTs can be challenging. Ancillary studies including ALK IHC, FISH, and NGS are helpful to establish diagnosis and to discover novel gene rearrangement potentially for targeted therapy.

Keywords Uterus · Inflammatory myofibroblastic tumors · ROS1 · ALK · Gene rearrangement

Introduction

Inflammatory myofibroblastic tumor (IMT) is a rare neoplasm composed of myofibroblastic and fibroblastic spindle cells with a background of mixed inflammatory cells [1]. It is extremely rare in the female genital tract [1–4]. Similar to IMTs in other anatomic sites, most IMTs in the uterus demonstrate indolent behavior, while a subset of uterine IMT with aggressive biological behavior has been described [2, 5, 6]. Although smooth muscle and endometrial stromal tumors are most common uterine mesenchymal neoplasms, morphologic and immunophenotypic overlaps between them and IMTs lead to diagnostic challenge. Approximately half of all IMTs harbor fusions of the anaplastic lymphoma kinase (ALK) gene at 2p23 [7] which may be susceptible to targeted therapy. Recently in IMTs, translocations of genes encoding

Lili Zhang and Lijuan Luan contributed equally to this work.

✉ Chen Xu
xu.chen@zs-hospital.sh.cn

✉ Yingyong Hou
houyingyong@aliyun.com

[1] Department of Pathology, Zhongshan Hospital, Fudan University, Shanghai 200032, People's Republic of China

[2] Geneseeq Research Institute, Nanjing Geneseeq Technology Inc, Nanjing, Jiangsu, People's Republic of China

[3] School of Public Health, Nanjing Medical University, Nanjing, People's Republic of China

other tyrosine kinases including ROS1, NTRK3, PDGFRb, and RET may also be therapeutically targetable [3, 7–10]. Therefore, identification of uterine IMTs demonstrates clinical importance as patients with IMTs may benefit from targeted therapy.

Here we present a series of 4 uterine mesenchymal tumor cases with aggressive behavior, initially diagnosed as leiomyosarcoma, demonstrating ALK or ROS1 rearrangements. Besides *TNS1-ALK* gene fusion, novel *ROS1-NUDCD3* and *NRP2-ALK* fusions were identified by next-generation sequencing (NGS). Finding of specific gene rearrangement suggested uterine IMTs may be more common than expected.

Materials and methods

Four consulting cases of primary uterine IMTs were acquired from the achieves of Department of Pathology, Zhongshan Hospital, Fudan University. All four patients received surgery resection as the primary treatment in other hospitals and came to our hospital for further treatment recommendations. Hematoxylin and eosin (H&E)-stained slides and immunohistochemical (IHC) stains of the primary tumors were available for all cases, and tissue from the recurrent tumors was available in 3 cases. H&E-stained sections and immunohistochemistry of all cases were reviewed by two pathologists (Lili Zhang and Lijuan Luan) to confirm the diagnosis. Details of treatment and follow-up were obtained from the institutional medical records or from contributing pathologists.

Immunochemistry

IHC staining was performed on a Dako or VENTANA Autostainer following the manufacturer's instructions. Primary antibodies are listed as follows: smooth muscle actin (clone 1A4, 1:100 dilution, Thermo), desmin (D33, ready-to-use, Dako), CD10 (56C6, 1:300 dilution, Leica Biosystems), ALK (D5F3, ready-to-use, Roche), ER (6F11, 1:80 dilution, Leica Biosystems), PR (16, 1:100, Leica Biosystems), cyclin D1 (EPR2241, 1:100 dilution, Abcam), ROS1 (D4D6, 1:250 dilution, Cell Signaling Technology).

Fluorescence in situ hybridization (FISH)

FISH on interphase nuclei from paraffin-embedded 4-micron sections was performed applying commercial available break-apart probes (ALK (2p23) Probe, lot: F.01330–01; ROS1 (6q22) Probe, lot: F.01086; Ret (10q11) Probe, lot: F.01104–01; YWHAE (17p13) Probe, lot: F.01183–01; JAZF1 (7p15) Probe, lot: F.01352–01; BCOR (Xp11) Probe, lot: F.01220–01, LBP Medicine Science and Technology Company, LTD, Guangzhou, China) according to manufacturer's instructions. In short, slides of tumor sections were deparaffinized, pretreated, and hybridized with denatured probes overnight, followed by post-hybridization washes and interphase nucleus counter staining with DAPI. Microscopic analysis was performed using a Leica DM6000B microscope (Leica Microsystems, Wetzlar, Germany) by Leica DFC310 FX imaging system. FISH images were processed by the LAS V4.5 (Leica Microsystems) software. For examination, at least 100 nonoverlapping tumor nuclei were analyzed. Gene rearrangement was considered if $\geq 15\%$ of tumor nuclei demonstrated break-apart signals.

Next-generation sequencing

Primary tumor samples of two patients (cases 1 and 3) and recurrence tumor samples of 3 patients (Case 1, 2 and 4) were targeted-sequenced by the GeneseeqOne™ pancancer gene panel (425-cancer-relevant genes, Geneseeq Technology Inc.). Briefly, for the formalin-fixed paraffin-embedded samples, five 10-μm tumor slices were used for DNA extraction using the QIAamp DNA FFPE Kit (QIAGEN, Valencia, CA, USA) following the manufacturer's instructions. DNA quality was assessed by spectrophotometry with absorbance at 230, 260, and 280 nm, and quantified by Qubit 2.0. Libraries were prepared by 1 μg of fragmented genomic DNA underwent end-repairing, A-tailing and ligation with indexed adapters sequentially, followed by size selection using Agencourt AMPure XP beads (Beckman Coulter). Hybridization-based target enrichment was carried out with GeneseeqOne™ pancancer gene panel (425-cancer-relevant genes, Geneseeq Technology Inc.), and xGen Lockdown Hybridization and Wash Reagents Kit (Integrated DNA Technologies). Captured libraries by Dynabeads M-270 (Life Technologies) were amplified in KAPA HiFi HotStart ReadyMix (KAPA Biosystems) and quantified by qPCR using the KAPA Library Quantification kit (KAPA Biosystems). Target enriched libraries were sequenced on the HiSeq4000 platform (Illumina) with 2×150 bp pair-end reads. Sequencing data were demultiplexed by bcl2fastq (v2.19), analyzed by Trimmomatic to remove low-quality (quality < 15) or N bases, and mapped to the reference hg19 genome (Human Genome version 19) using the Burrows-Wheeler Aligner. PCR duplicates were removed by Picard (available at: https://broadinstitute.github.io/picard/). The Genome Analysis Toolkit (GATK) was used to perform local realignments around indels and base quality reassurance. SNPs and indels were called by VarScan2 and HaplotypeCaller/UnifiedGenotyper in GATK, with the mutant allele frequency (MAF) cutoff as 0.5% for tissue samples and a minimum of three unique mutant reads. Gene fusions were identified by FACTERA and copy number variations (CNVs) were analyzed with ADTEx.

Results

Main clinicopathological parameters were summarized in Table 1. Patient age was 53, 51, 64, and 44 years respectively. Two patients (cases 1 and 3) presented with abnormal painless vaginal bleeding. In three cases, the primary tumors located in the uterus body. Cases 1 and 2 demonstrated multiple masses with the largest lesion 54 mm and 88 mm in diameter, respectively. Histologically, in case 1, case 2, and case 4, tumor cells were spindled containing eosinophilic cytoplasm and elongated nuclei in fascicular arrangement with mild to moderate nuclear atypia. In case 3, nuclear atypia was moderate to severe with multinucleated and bizarre cells. Necrosis was identified in cases 1 and 3. Prominent inflammatory cell infiltration was present in one tumor (case 2), while scant inflammatory cells were found in the other three tumors (cases 1, 3, and 4). Immunochemically, smooth muscle markers (a-SMA, desmin) were positive in all four tumors; CD10 was diffusely positive in case 1, partially positive in cases 3 and 4 and negative in case 2; ALK was positive in three tumors (cases 2, 3, and 4), while negative in one tumor (case 1). FISH analysis for ALK rearrangements was performed in all four cases and was positive in three tumors (cases 2, 3, and 4). ROS1 rearrangement was identified in case 1. NGS results demonstrated two novel fusions including *NUDCD3-ROS1* (*NUDCD3: exon2-ROS1: exon36*) fusion (case 1) and *NRP2-ALK (NRP2: exon8-ALK: exon19)* fusion (case 2); and previously reported *TNS1-ALK* fusion *(TNS1: exon16-ALK:exon18)* fusion (case 3) and *TNS1: exon19-ALK: exon12* (case 4). With regard to treatment, four patients received surgery as primary treatment and following adjuvant treatments: chemotherapy (3 patients), chemotherapy and targeted therapy (case 1), targeted therapy (case 4), and reoperation (cases 1, 2, and 4). Recurrences occurred in all 4 patients, and time to recurrence ranged from 1 month to 7 years. Follow-up ranged from 5 months to 15 years. Two patients were alive with disease (cases 1 and 3), and the other 2 patients died of disease progression (cases 2 and 4).

Clinicopathologic details of each case are presented as follows.

Table 1 Clinicopathologic features of uterine IMTs

Case	Age	Location	Recurrence and/or metastasis (mos)	Follow-up (mos)	Status	Size (mm)	Margin	Necrosis	Atypia	IHC			ALK FISH	Gene fusions
										SMA	CD10	ALK		
1	53	Corpus	Y (5)	19	AWD	Multiple (largest 54)	Inf	Pres	Mi-Mo	Pos	Pos	Neg	Neg	*NUDCD3*:exon2-*ROS1*:exon36
2	51	Corpus	Y (9)	12	DOD	NA	NA	NA	Mi	Pos	Neg	Pos	Pos	*NRP2*:exon8-*ALK*:exon19
3	64	Corpus	Y (1)	5	AWD	Multiple (largest 88)	NA	Pres	Mo-Se	Pos	Pos	Pos	Pos	*TNS1*:exon16-*ALK*:exon18
4	44	Corpus	Y (7 years)	15 years and 10 mos	DOD	NA	NA	NA	Mi	Pos	Pos	Pos	Pos	*TNS1:exon19-ALK:exon12*

mos, months; *Y*, yes; *NA*, not available; *DOD*, died of disease; *AWD*, alive with disease; *Inf*, infiltrated; *Pres*, present; *Mi*, mild; *Mo*, moderate; *Se*, severe

Case presentations

Case 1

A 53-year-old female patient went to hospital for abnormal menstruation in February 2020. Ultrasound showed multiple heterogeneous hypoechoic masses in the wall of uterus, among which the largest was 54×41 mm in size. She was admitted to

hospital with abnormal vaginal bleeding for 17 days and anemia in July 2020. Gynecological examination found uterus enlargement as 3 months pregnancy. She underwent laparoscopic total hysterectomy combined with bilateral adnexectomy, pelvic lymphadenectomy, and pelvic adhesiolysis.

Gross examination revealed multiple masses in the uterus wall. The largest mass was 8 cm in diameter, poorly circumscribed, gray-white with partial necrosis, and fish-flush cut surface. The initial pathological diagnose was uterine leiomyosarcoma.

In August 2020, the patient accepted 4 cycles of chemotherapy (gemcitabine + docetaxel). Five months after surgery in December 2020, FDG-PET/CT showed metastatic nodules in liver surface, pelvic omentum, and mesentery. The patient was referred to our hospital and treated by palliative chemotherapy (dacarbazine + domesol + arotinib) since Jan 2021. After 2 months' treatment, the patient achieved partial regression (PR).

During pathological consultation, histology of the primary tumor was under re-evaluation. Generally, the tumor showed infiltrative margins, composed of fascicular spindle cells with hypercellular area alternating with hypocellular region (Fig. 1A). Tumor cells were spindle with eosinophilic cytoplasm and elongated nuclei. Nuclear atypia was mild to moderate, while in some areas multinucleated cells and necrosis was observed. Mitoses count was approximately 10/10 HPF (Fig. 1B). Infiltration of inflammatory cells was not prominent. Immunochemically, tumor cells were positive for smooth muscle markers, including a-SMA and desmin (Fig. 2A), as well as CD10, ER, and PR. They were negative for ALK, ROS1, and CyclinD1. For differential diagnosis, FISH analysis was used to evaluate *ALK*, *ROS1*, *JAZF1*, *YWHAE*, and *BCOR*. FISH results demonstrated the tumor was positive for ROS1 rearrangement in 40% tumor cell, and negative for the other 4 genes (Fig. 3A). Moreover, subsequent NGS analysis revealed a *NUDCD3-ROS1* (*NUDCD3: exon2-ROS1: exon36*, AF 21.40%) fusion (Fig. 4A). The diagnosis of IMT was established.

The patient continued chemotherapy (dacarbazine + domesol + arotinib) until May 2021. In June 2021,

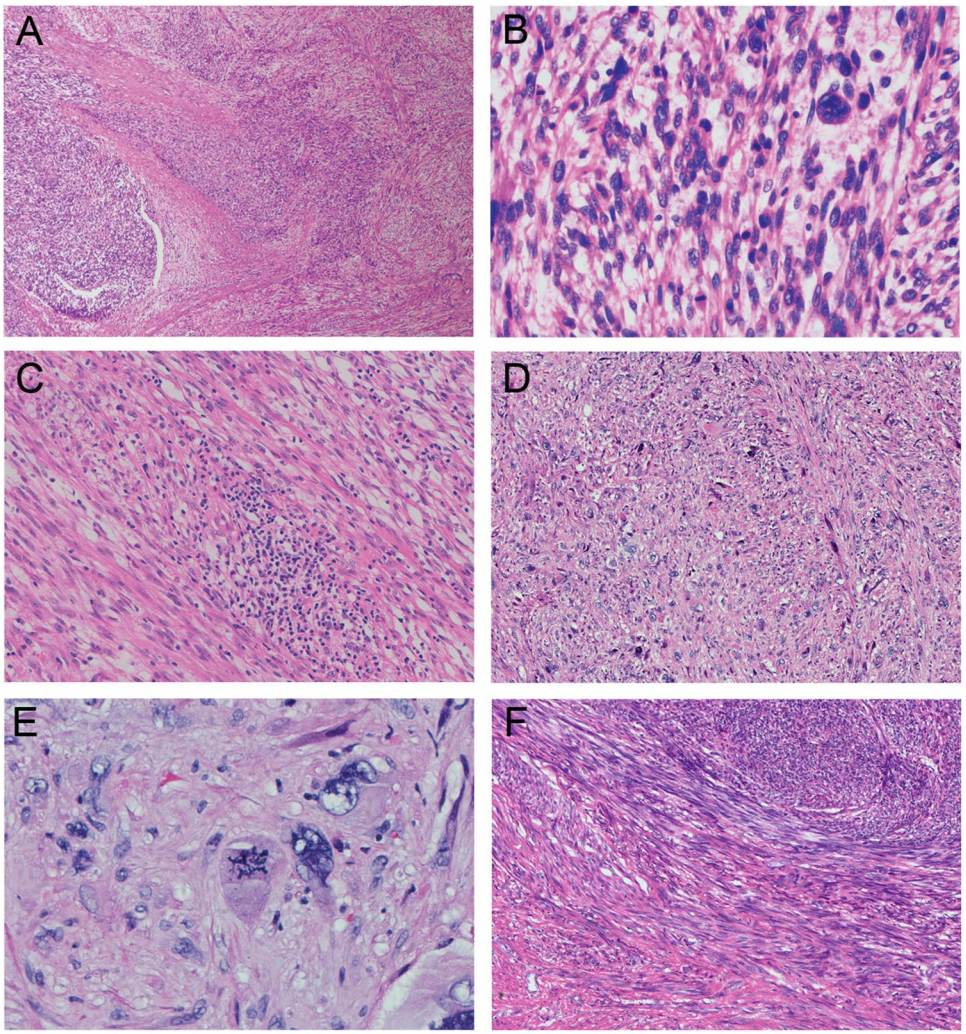

Fig. 1 Tumor cells are spindled containing eosinophilic cytoplasm and elongated nuclei, which is composed of fascicular spindled cells with hypercellular area alternating with hypocellular region (×4) (case 1; **A**). Hypercellular region with mitoses and multinucleated cells at ×400 (case 1; **B**). Spindled tumor cells in fascicular arrangement, while inflammatory cell infiltration is present (×200) (case 2; **C**). Spindled and epithelioid tumor cells (×100) (case 3; **D**). Bizarre and multinucleated cells with mitoses (×400) (case 3; **E**). Infiltrative tumors showed percolation of tumor cells into the myometrium (×100) (case 4; **F**)

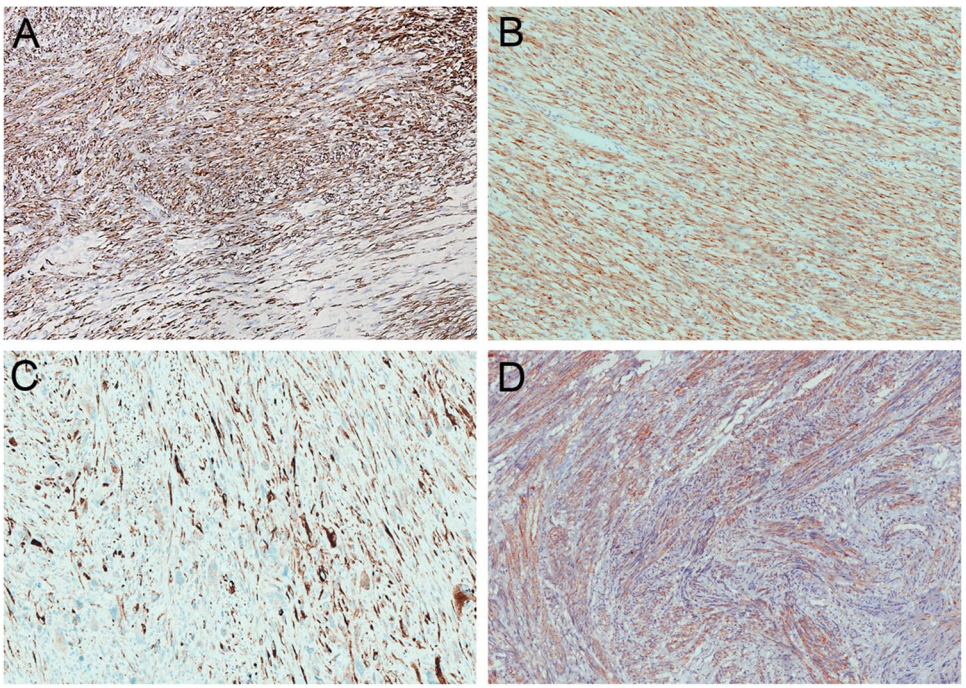

Fig. 2 Tumor cells positive for desmin (case 1; **A**). Tumors showing a granular cytoplasmic and perinuclear ALK staining pattern (case 2; **B**, case 3; **C**, and case 4; **D**)

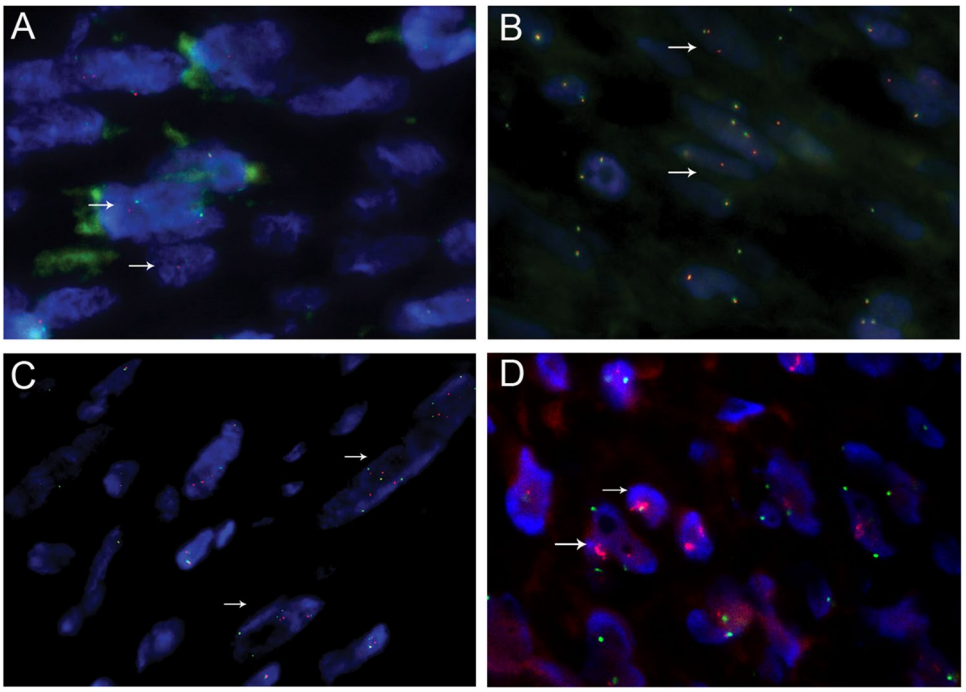

Fig. 3 Positive results detected by break-apart FISH showing ROS1 (case 1; **A**) and ALK rearrangement (case 2; **B** and case 3; **C**). MDM2 amplification of case 4 (**D**)

the patient achieved continuous partial remission (PR). Considering ROS1 gene fusion as a target, the patient was given crizotinib for maintenance treatment. After 25 days on crizotinib, CT scan indicated progressive disease. She switched back to chemotherapy (dacarbazine + domesol + arotinib). On July 27th, she developed further progressive disease and a post-line regimen of arotinib + eribulin + Keytruda was introduced. Chemotherapy was paused due to increase of creatinine. In September 2021, pelvic lesion resection combined with right hemicolectomy, partial rectal resection, descending colostomy, vaginal stump formation, and complex intestinal adhesion lysis were performed. The patient was alive with disease at last follow-up (17 months after the first operation).

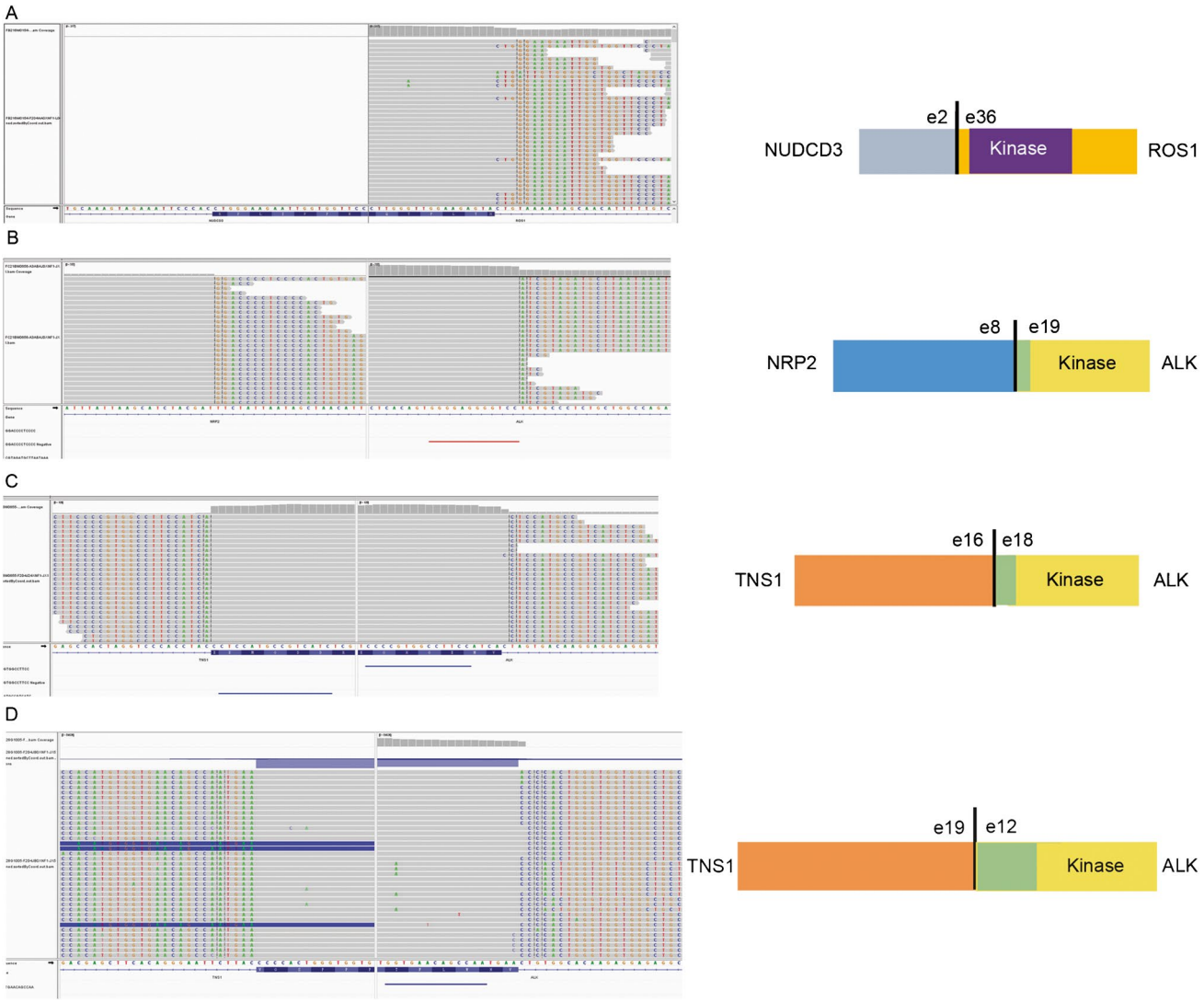

Fig. 4 NGS showing *NUDCD3-ROS1* fusion (*NUDCD3: exon2-ROS1:exon36*, AF 21.4%) (case 1; **A**), *NRP2-ALK* fusion (*NRP2*:exon8-*ALK*:exon19, AF 64.1%) (case 2; **B**), *TNS1-ALK* fusion (*TNS1*:exon16-*ALK*:exon18, AF 30.36%) (case 3; **C**), and *TNS1-ALK* fusion (*TNS1: exon19-ALK: exon 12*, AF 86.29) (case 4; **D**)

Case 2

A 51-year-old female was admitted to hospital in June 2021 due to failure of stool and gas pass for 1 week, accompanied by lower abdominal pain, abdominal distension without chills, and high fever. PET-CT examination showed multiple low-density foci in pelvic and peritoneal cavity with elevated FDG, considering metastasis as well as multiple nodules in both lungs with partial increase of FDG. She had a history of "uterine smooth muscle sarcoma" and underwent total hysterectomy combined with double adnexectomy in September 2020.

To relief intestinal obstruction, excision of pelvic and abdominal lesions, partial resection of small intestine, and enterostomy were performed on June 24th 2021. Gross examination revealed multiple masses with fish-flesh cut surface, which was prone to bleed. Histologically, tumor cells were spindled with eosinophilic cytoplasm and elongated nuclei in fascicular arrangement (Fig. 1C). Nuclear atypia was mild to moderate. Mitoses were observed (9/10 HPF). Inflammatory cell infiltration was seen in some areas of stroma (Fig. 1C). IHC showed positive expression of SMA and desmin while negative for CD10. Tumor cells were strongly and diffusely positive for ALK protein (Fig. 2B). FISH analysis revealed 60% of tumor cells with isolated red signal (Fig. 3B). NGS analysis identified a *NRP2-ALK* fusion (*NRP2*: exon8-*ALK*: exon19, AF 64.11%) (Fig. 4B). After consultation, the initial diagnosis of smooth muscle sarcoma was corrected to IMT. The patient died of disease progression in September 2021 after adjuvant chemotherapy (specific drug unknown).

Case 3

A 64-year-old female presented with painless vaginal bleeding for a month. She went to a local hospital in July 2021, and ultrasound analysis showed multiple uterine intramural myoma with the largest 88 × 74 × 88 mm in size. The patient has a 20 years history of uterine fibroids. She underwent laparoscopic total hysterectomy with bilateral adnexectomy on September 22nd 2021 in the local hospital. Grossly, the uterus was broken with necrosis, which was difficult to measure. Initial diagnosis favored leiomyosarcoma. On Oct 27th 2021, PET-CT scan revealed right upper lung metastasis. The patient was referred to our hospital and treated by palliative chemotherapy (dacarbazine + epirubicin).

Sections of the primary tumor were sent to our hospital for pathological consultation. Histologically, tumor cells were densely composed of spindled and epithelioid cells with eosinophilic cytoplasm. Nuclear atypia was moderate to severe, while multinucleated and bizarre cells could easily be seen (Fig. 1D). Mitoses were 5–6/10 HPF (Fig. 1E). Inflammatory cells were scant. Immunochemically, tumor cells expressed smooth muscle markers including SMA and desmin. ALK staining was diffusely positive (Fig. 2C). ALK FISH analysis confirmed ALK translocation in 70% of the tumor cells (Fig. 3C). NGS analysis showed *TNS1-ALK* fusion (*TNS1*: exon16-*ALK*: exon18, AF 30.36%) (Fig. 4C). Therefore, the initial diagnosis was corrected to uterine IMT.

The patient achieved partial response (PR) after 4 cycles of chemotherapy. She was alive with disease at last follow-up (5 months after the first operation).

Case 4

A 59-year-old female was admitted to hospital in March 2018 because of retroperitoneal tumor for 1 year with pain of both lower limbs for a month. The lesion was diagnosed as smooth muscle tumor by biopsy in another hospital. She had a history of "uterine myoma" in November 2003, and "smooth muscle tumor of undetermined significance" of the right ovary in October 2010. The patient received apatinib treatment from May 2017 and had disease progression after 8 months.

In pathological consultation, the slides of uterine and ovarian tumor were reviewed. Histologically, tumor cells in the uterus were spindled in fascicular arrangement with mild nuclear atypia, while mitosis was scarcely observed (Fig. 1F). In the meanwhile, ovarian tumor was more cellular with mild to moderate nuclear atypia and brisker mitosis (12/50 HPF). Both uterine and ovarian tumor cells expressed SMA, desmin, and CD10, as well as ALK (Fig. 2D). ALK translocation was confirmed by FISH analysis. The diagnosis of the uterine and ovarian tumors was corrected to IMT.

In order to relieve compression of the retroperitoneal tumor, the patient underwent retroperitoneal lesion resection in February 2018. Gross examination revealed one enveloped gray and brown tumor with fish-flesh cut surface, size 15 × 14 × 4 cm. Grayish yellow necrosis was seen in some areas. Histologically, tumor cells showed similar features to primary uterine tumor but with more severe nuclear atypia and brisk mitosis (38/50 HPF). IHC results revealed SMA, desmin, CD10, and ALK expression. ALK translocation in 80% of the tumor cells and MDM2 amplification were confirmed by FISH (Fig. 3D). NGS analysis identified TNS1-ALK fusion (TNS1: exon19-ALK: exon12, AF 86.29%) (Fig. 4D). After 5 months after surgery, CT scan follow-up showed multiple recurrence lesions in pelvic and peritoneal cavity, along with left lung metastasis. The patient received crizotinib targeted therapy since then. After 2 months of crizotinib treatment, she developed further progressive disease and was treated with alectinib instead. The patient stayed SD (stable disease) for 4 months with alectinib treatment. She died of disease progression in September 2019.

Mutation profiles

We investigated the genetic profiles of all four cases, including post-crizotinib (RC) samples of two cases (case 1 and case 4). Top 30 gene mutations and somatic copy number variants of four patients were shown in Fig. 5A. Cell cycle and p53 signaling pathway related gene aberrations (*TP53*, *MYC*, *MDM2*, *CDK4*, *CDKN2A*) were identified in all the 4 cases. In case 1, mutations including hotspot *TP53(p.E258K)*, *TP53(p. L252del)*, *ATRX(p. M1556Nfs*22)*, and *NUDCD3:exon2-ROS1:exon36* were identified both tumors before and post crizotinib treatment. However, *MYC* copy number gain was found only in tumor before treatment, Moreover, *THADA* gene fusion and other mutations were only found in the recurrent tumors after crizotinib treatment (Fig. 5A case 1, RC1-4). In case 4, *CDK4(AMP)*, *MDM2(AMP)*, *CDKN2A(DEL)* together with *TNS1:exon19 ~ ALK:exon12* were identified in tumors before and post crizotinib treatment. Hotspot *TP53 (p.C238Y)* was identified in case 3, and *IGR (upstream DMRTA1)-CDKN2A:exon2* was found in case 4. Generally, besides ALK translocation, the 4 cases shared limited gene aberrations. The multiple gene alterations in the 4 cases indicated that the IMT was a heterogenous entity. To understand the biological importance of the mutations, we performed the KEGG pathway analyses of mutated genes of 4 patients. We found that despite of diversity in the altered genes, these aberrations mainly involve several enriched pathways include the PI3K-Akt signaling pathway, MAPK signaling pathway, and RAS signaling pathway as shown in Fig. 5B.

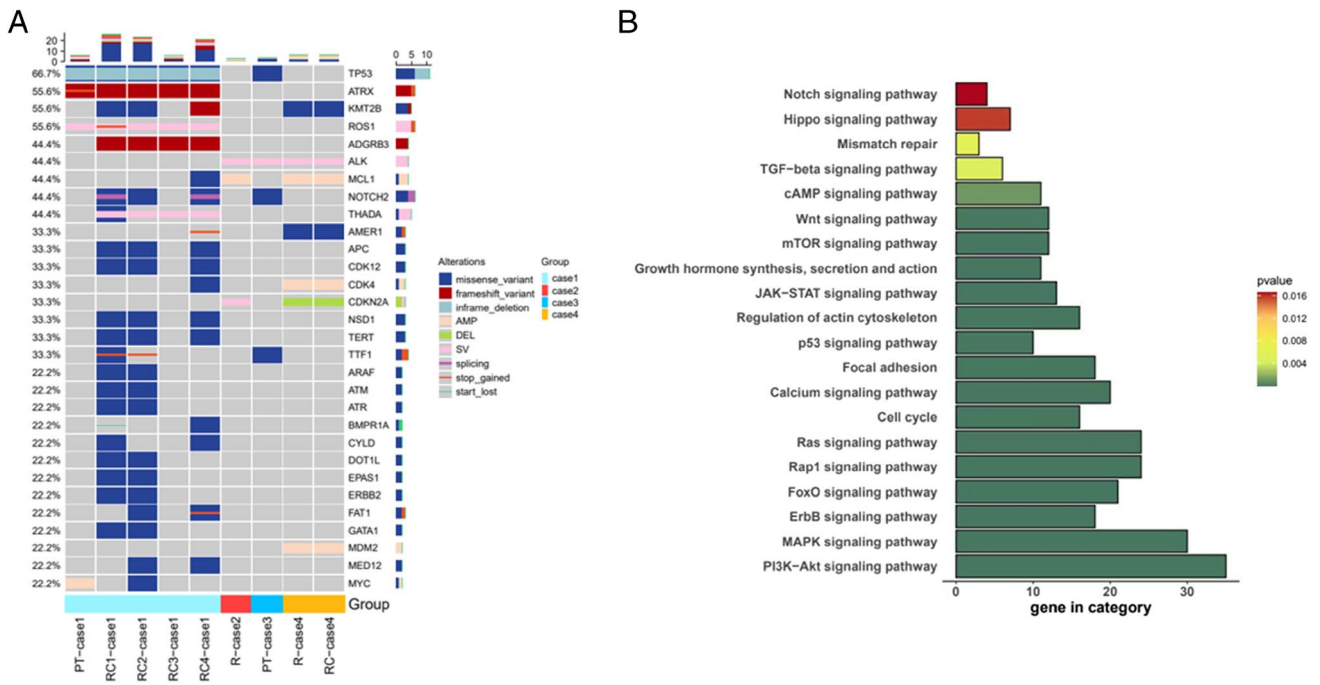

Fig. 5 Genetic alteration and somatic copy number variants of uterine IMTs from primary tumor (PT), recurrences (R), and recurrences after crizotinib (RC) (**A**). KEGG pathway analyses of mutated genes of 4 patients with inflammatory myofibroblastic tumor (**B**)

Discussion

In this article, we presented 4 uterine IMTs with novel gene fusions. IMT is a mesenchymal neoplasm of intermediate biologic potential, which occurs mostly in the lung and abdomen cavity [1]. Histologically, it is characterized as a neoplasm composed of myofibroblastic and fibroblastic spindle cells with a background of mixed inflammatory cells [1].

IMTs rarely arise from the uterus or cervix. Less than 150 uterine IMTs were reported in the English literatures [2–39]. Clinicopathologic features of these cases were summarized in Table 2. The age at presentation of the reported cases ranged from 3.5 to 78 years, with median age of 39 years old. About 70% (96/126) of the cases are arising from the uterus body; 15% (19/126) cases affect cervix. There were 33 IMT cases associated with the placenta during pregnancy [5, 8, 9, 12, 14, 20, 26]. Uterine IMTs can be single or multiple mass. Tumor size ranged from 5 to 200 mm (median, 45 mm). The margins of tumors are described in 77 cases, from which about half of the tumors are well circumscribed (37/77), the others are infiltrated (28/77), irregular (9/77), and pushing (3/77).

Histologically, IMTs are typically consisted of fibroblastic/myofibroblastic spindle cells in a myxoid background which is accompanied by inflammatory infiltrates, including lymphocytes, plasma cells, foamy histiocytes, neutrophils, and eosinophils. There are three histologic patterns described in the literature: (1) a hypocellular/loose myxoid pattern; (2) a hypercellular/compact pattern, characterized by cellular areas arranged in fascicular or storiform architecture; and (3) a hyalinized pattern, composed of loosely arranged tumor cells in an abundant collagenous matrix. Nuclear atypia is at most mild, and the mitotic index is usually low (mostly less than 5/10 HPF). Three of our cases have features consistent with the pattern 2, while the fourth case was densely composed of spindled and epithelioid cells with multinucleated and bizarre cells. Nuclear atypia in our cases was moderate to severe. Only one case showed prominent inflammatory cells, making it difficult to make a differential diagnosis with smooth muscle tumors.

Immunochemically, IMTs variably express SMA, actin, desmin, and CD10. Usually the extent and density of smooth muscle markers is not as strong as smooth muscle tumors. In this study, all the 4 cases showed strong and diffuse IHC staining of SMA and desmin. These IHC findings and histological features were the main reasons leading to the misdiagnosis of leiomyosarcoma. Studies showed that the expression of smooth muscle makers in uterine IMT was inversely correlated to the degree of myxoid stroma [14]. Tumors with more myxoid stroma are less likely to show smooth muscle expression compared with more cellular areas with less myxoid stroma.

In the literatures, ALK protein expression is observed in about 87% (103/119) of uterine IMTs, However, one ALK IHC negative case was identified ALK rearrangement by FISH [2]. Several gene fusion partners for *ALK* have been

Table 2 Clinical, histologic, and molecular features of uterine IMTs reported in the literature

References	# of cases	Age	Location	Recurrence and/or metastasis	Follow-up (mos)	Status	Size (mm)	Margin	Necrosis	Atypia	IHC			ALK FISH
											SMA	CD10	ALK	
Gilks et al. [38]	2	6, 30	Corpus	No	60, 52	NED	130, 40	Cir	Abs	Nil	NA	NA	NA	NA
Abenoza et al. [37]	1	58	Cervix	No	6	NED	17	Cir	Abs	Nil	NA	NA	NA	NA
Kargi et al. [36]	1	53	Corpus	No	24	NED	NA	NA	NA	NA	NA	NA	NA	NA
Azuno et al. [35]	1	66	Corpus	No	52	NED	50	Cir	NA	NA	Neg	NA	Pos	NA
Rabban et al. [32]	6	6–46	Corpus	No	1.5–5	NED (4) NA (2)	10–120	Pu (3) FI (3)	Abs	Nil	NA	NA	Pos (5) NA (1)	NA
Gucer et al. [33]	1	48	Cervical stroma, bilateral parametria, subepithelial tissues of the vagina	No	8	NED	50	Inf	NA	Mi	Neg	NA	NA	NA
Shintaku and Fukushima [31]	1	63	Corpus	No	8	NED	110	Inf	Pres	Mi	Pos	Neg	NA	NA
Gupta et al. [30]	1	14	Corpus	No	12	NED	110	Cir	Abs	Nil	NA	NA	NA	NA
Olgan et al. [29]	1	28	Corpus	No	12	NED	20	Reg	Abs	Mi-Mo	NA	Pos	Pos	NA
Fuehrer et al. [28]	7	26–52	Corpus (5) Cervix (2)	NA	NA	NA	NA	NA	NA	Nil (2) Mi (5)	Pos (4) Neg (2) NA (1)	Pos (4) Neg (1) NA (2)	Pos (6) Neg (1)	Pos (5) Neg (2)
Kushnir et al. [27]	1	30	Corpus	No	6	NED	Multiple Largest 53	Inf	NA	Mi	Neg	NA	Neg	NA
Parra-Herran et al. [6]	10	29–73	Corpus (9) Cervix (1)	Yes (2) No (4) NA (4)	6–36	NED (4) AWD (2) NA (4)	11–195	Cir (4) Inf (5) NA (1)	Abs (7) Pres (3)	Mi (7) Mo (3)	Pos (8) Neg (1) NA (1)	Pos (6) NA (4)	Pos (8) NA (2)	Pos (8) NA (2)
Subbiah et al. [23]	1	50	Corpus	Yes	24	AWD	NA	Inf	NA	NA	NA	NA	Pos	NA
Fraggetta et al. [25]	1	10	Cervix	No	80	NED	20	Cir	Abs	Nil	Pos	NA	Pos	Pos
Banet et al. [26]	2	30, 33	Placental disk	No, NA	3 weeks, NA	NED, NA	33, 20	Cir	Abs	M	Neg, NA	Pos	Neg, Pos	Neg, NA
Saeed et al. [24]	1	26	Placental disk	NA	5	NA	NA	Ire	Abs	M	NA	NA	Pos	NA

Table 2 (continued)

References	# of cases	Age	Location	Recurrence and/or metastasis	Follow-up (mos)	Status	Size (mm)	Margin	Necrosis	Atypia	IHC			ALK FISH
											SMA	CD10	ALK	
School-meester et al. [6]	4	53–56	Corpus	Yes (2) NA (2)	27, 48, NA (2)	DOD (2) NA (2)	35–140	Inf (2)	Abs	M (2) Mo (2)	Pos (3) Neg (1)	Pos (2) Neg (2)	Pos	Pos (2) Neg (1) NA (1)
Pickett et al. [20]	5	37–47	Corpus	No (4) NA (1)	74, 30, 4, 66, NA	NED (4) NA (1)	17–190	Cir (3) Inf (1) NA (1)	Abs (4) Equi (1)	Nil (3) Mi (2)	Pos	Pos (2) Neg (3)	Pos	Pos
Haimes et al. [4]	12	24–78	Corpus	No (11) NA (1)	9–93 NA (1)	NED (11) NA (1)	18–150	NA	Abs (11) Pres (1)	Mi	Pos	NA	Pos (11) Neg (1)	Pos (4) Neg (3) Fail (1) NA (4)
Bennett et al. [5]	13	8–63	Corpus	No (8) Yes (4) NA (1)	1–132 NA (1)	NED (8) DOD (3) AWD (1) NA (1)	25–200	Inf (6) FI (2) NA (5)	Pres (8)	Mi (6) Mo (5) Se (2)	NA	Pos (11) Neg (1) NA (1)	Pos (12) Neg (1)	Pos (8) Abn (1) Neg (1) NA (2) Failed (1)
Takahashi et al. [10]	1	44	Corpus	No	31	NED	72	NA	Abs	NA	Neg	Neg	Neg	Neg
Ladwig et al. [19]	2	44, NA	Corpus, placenta disk	No (1) NA (1)	30 weeks, NA	NED, NA	68, 15	Cir, NA	Pres (1)	Minimal	NA	Pos, NA	Pos	Pos
Squires et al. [17]	1	28	Fetal membrane	NA	NA	NA	35	Cir	Abs	Nil	NA	NA	Pos	NA
Mohammad et al. [18]	3	53, 24, 31	Corpus	NA	NA	NA	NA	NA	NA	Mi	NA	NA	Pos	NA
Lee et al. [16]	1	39	Corpus	Yes	48	AWD	NA	NA	NA	NA	NA	NA	NA	NA
Stikova et al. [15]	1	66	Corpus	Yes	A few months	DOD	NA	Inf	Pres	Se	NA	NA	Pos	NA
Cheek et al. [9]	6	25–41	Corpus	No (3), NA (2)	5, 19, Resent case, NA (3)	NED (2), Resent, NA (3)	15–90	NA	Pres (2)	Mi-Mo	NA	NA	Pos (5), Neg (1)	Pos (3) Neg (1) NA (2)
School-meester et al. [8]	1	39	Membranous decidua	NA	NA	NA	65	Cir	Abs	Mi	NA	NA	Neg	Neg
Makhdoum et al. [12]	9	21–41	Fetal membrane (4) Placenta disk (3) Corpus (2)	No (1) NA (8)	6 weeks NA (8)	NED (1) NA (8)	20–60	Cir (5) SM (2) I (2)	Pres (5)	Nil (3) No (2) Mi (4)	Pos (5) Neg (1) NA (3)	Pos	Pos (7) Neg (2)	Pos (6) Neg (2) Failed (1)

Table 2 (continued)

References	# of cases	Age	Location	Recurrence and/or metastasis	Follow-up (mos)	Status	Size (mm)	Margin	Necrosis	Atypia	IHC			ALK FISH
											SMA	CD10	ALK	
Devereaux et al. [14]	8	23–42	Corpus (1) Placenta disk (1) Extrapla-cental fetal membranes (1) Detached (5)	No (4) NA (4)	8–26, NA (4)	NED (4) NA (4)	20–60	Cir (7) NA (1)	Pres (2)	Mi	Pos (6) Neg (2)	Pos	Pos (7) Neg (1)	Pos (7) Neg (1)
Zarei et al. [11]	1	29	Corpus	No	12	NED	35	Cir	Abs	Nil	Pos	NA	Pos	Pos
Etlinger et al. [13]	1	3.5	Corpus	No	36	NED	30	I	Abs	Mi	Pos	NA	Pos	Pos
Collins et al. [2]	9	32–64	Corpus	Yes	12–101	AWD (6) DOD (3)	6–150	Cir (2) Inf (7)	Pres (5)	Mi-Se	Pos (4) Neg (2) NA (3)	NA	Pos (8) Neg (1)	Pos (4) NA (5)
Bennett et al. [3]	1	43	Corpus	NA	NA	NA	Multiple masses, largest 30	Cir	Abs	Mi	NA	Pos	Neg	NA
Kuisma et al. [39]	9	36–48	Corpus	No	41–91	NED	15–90	Cir (2) NA (7)	Abs	Mi	NA	Pos (3) Neg (6)	Pos (7) Neg (1) NA (1)	NA

NA, not available; *NED*, no evidence of disease; *DOD*, died of disease; *AWD*, alive with disease; *Cir*, circumscribed; *Pu*, pushing; *I*, irregular; *FI*, focally irregular; *Inf*, infiltrated; *Reg*, regular; *SM*, separate mass; *Pres*, present; *Abs*, absent; *Equi*, equivocal; *Mi*, mild; *Mo*, moderate; *Se*, severe; *Pos*, positive; *Neg*, negative; *Abn*, abnormal; *NI*, not identified

reported in uterine IMTs (Table 3) including *TIPM3(16)*, *THBS1(12)*, *IGFBP5(10)*, *FN1(3)*, *TNS1(5)*, *DES (3)*, *DCTN1(2)*, and *RANBP2(1)* [3–5, 9, 11, 12, 14–16, 18, 23]. Recently, although rare, alternative translocations including *ROS1* (2 cases, *TIMP3-ROS1*, *FN1-ROS1*), *RET* (2 cases, *TIMP3-RET*, *SORBS1-RET*), *IGFBP5-PDGFRB* (1 case), and *NTRK3* (1 case, *NTRK3-ETV6*) have been identified in a subset of ALK-negative uterine IMT tumors [8–10, 39]. In the present study, novel *NUDCD3-ROS1* (case 1) and *NRP2-ALK* (case 2) fusions were identified for the first time. Beside *ALK* and *ROS1* gene status, we further investigated the genetic profiles of the 4 IMTs by NGS. We also compared the changes of mutations and copy number variation before and after crizotinib treatment. Notably, *TP53* mutations including a hotspot mutation *(p.E258K)* and *MYC* copy number gain were identified in case 1. However, patients harboring ROS1 fusion with concomitant *TP53* mutations or *MYC* overexpression may have influence on tyrosine kinase inhibitor (TKI) resistance in lung cancer [40, 41]. Moreover, it is reported in lung cancer that *MDM2* amplification plays an important role in TKI resistance [42], which may explain the failure of crizotinib treatment in case 4.

IMTs are considered to have intermediate biologic potential with a local recurrence and distant metastasis rate of about 25% [1]. In the reported uterine IMTs, most cases showed indolent behaviors without follow-up evidence of recurrence or metastasis. However, cases with aggressive behaviors in the uterus IMTs have been described [2, 5, 6, 15, 16, 19–23, 37]; the recurrence and metastasis rate is about 29% (22/77). Histologically, approximately 73% (16/22) aggressive tumors had infiltrative margins. Necrosis was more frequently seen in aggressive IMTs (10/22) than in indolent tumors [5, 6]. Aggressive biological behaviors may be related to tumor size, higher grade of atypia, and mitoses index [2, 5, 6]. In our study, all the four cases show aggressive behavior. Necrosis are seen in two cases, while mitoses index are relatively high in all four cases (> 5/10 HPF).

To better understand the underlying mechanism, we performed NGS analysis to the primary tumors of all the 4 cases and recurrent tumors from 2 cases. We identified different alterations in multiple genes. These findings supported IMT as a heterogenous entity. Despite of the diversity of gene mutations, several enriched pathways which involved in the IMTs include the PI3K-Akt signaling pathway, MAPK signaling pathway, and RAS signaling pathway were confirmed [43]. Furthermore, we discovered TP53 mutations, CDKN2A structure variation, and MDM2 amplification in the 4 cases. These alterations may lead

Table 3 Summary of reported gene rearrangements in uterine IMTs

Gene fusion	No. of cases	Identified fusion variants reported
TIMP3-ALK [4, 5, 9, 12, 14, 39]	16	TIMP3 (exon1)-ALK (exon19)/TIMP3 (exon1)-ALK (exon 20) TIMP3 (exon 1)-ALK (ALK exon 12)
THBS1-ALK [4, 5, 9, 14, 18]	12	THBS1 (exon 7)-ALK (exon 18) THBS1 (exon 4)-ALK (ALK exon 19) THBS1-ALK (ALK exon 17)
IGFBP5-ALK [2, 4, 5, 18, 39]	10	IGFBP5 (exon 1)-ALK (exon 19) IGFBP5 (exon 1)-ALK (exon 19)/IGFBP5 (exon 1)-ALK (exon 20)
FN1-ALK [2, 4]	3	FN1 (exon/intron 15)-ALK (exon 18)/FN1 (exon 15)-ALK (exon 19) FN1 (exon 27)-ALK (exon 18)/FN1 (exon 27)-ALK (exon 17)/FN1 (exon 27)-ALK (exon 19)
TNS1-ALK [2, 16, 18, 39]	5	
DES-ALK [5, 11]	3	DES (exon 6)-ALK (exon 20)
DCTN1-ALK [2, 23]	2	DCTN1 (exon 29)-ALK (exon 20)
PPP1CB-ALK [15]	1	
SYN3-ALK [12]	1	SYN3 (exon 1)-ALK (ALK exon 20)
RANBP2-ALK [2]	1	
SEC31-ALK [5]	1	
TNC-ALK [39]	1	
ETV6-NTRK3 [10]	1	
FN1-ROS1 [3]	1	FN1 (exon 37)-ROS1 (exon 34)
TIMP3-ROS1 [8]	1	TIMP3-ROS1 (ROS1 exon 35)
TIMP3-RET [9]	1	TIMP3-RET (RET exon 11)
SORBS1-RET [39]	1	
IGFBP5-PDGFRB [39]	1	

to activation of P53 signaling pathway which may play important roles in the adverse outcome of these uterine IMTs. Theses finding provided new insights to the understanding of this rare entity and the underlying mechanisms are to be further elucidated.

The main differential diagnosis of uterine IMTs is smooth muscle tumors due to morphologic and immunophenotypic overlap between the two entities. Parra-Herran et al. [22] reported 4 cases out of 30 cases previously diagnosed as uterine smooth muscle tumor to be IMTs with positive ALK IHC or FISH results. In the current cases, histologically, all the cases were indistinguishable from smooth muscle tumors due to lack of inflammatory cell infiltration, and were positive for smooth muscle markers such including SMA and desmin; therefore, all of them were initially diagnosed as smooth muscle tumors. The final diagnosis was established after the confirmation of ROS1 and ALK gene rearrangement. Thus, distinguishing uterus IMTs from smooth muscle tumors can be quite challenging especially for ALK negative IMTs. Ancillary modalities including IHC, FISH, and NGS may help to make the correct diagnosis and find gene rearrangement potentially for targeted therapy.

In conclusion, we presented 4 rare uterus IMTs with malignant biological behaviors and identified novel *NUDCD3-ROS1* and *NRP2-ALK* fusions. All these cases were misdiagnosed as smooth muscle tumors at beginning and correct diagnosis was established after ALK and ROS analysis in consultation, indicating great challenges in the pathology diagnosis of this rare entity. It might be reasonable to include ALK in the IHC panel for differential diagnosis of uterus mesenchymal tumors in routine practice. NGS analysis revealed certain gene alterations involved in the P53 pathway which may contributed to the malignant behaviors. These findings shed new lights on the understating of this rare entity, and further mechanism studies are expected.

Author contribution L.Z. and L.L. reviewed the H&E, IHC, and FISH results and drafted the manuscript. L.S., R.X., J.H., J.S., Y.H., Y.X., X.W., and Y.S. performed experiments and analyzed data. J.Y., Y.H., and C.X. interpreted results and revised the manuscript. L.Z., L.L., Y.H., and C.X. are guarantors of this work and, as such, had full access to all the data in the study and take responsibility for the integrity of the data and the accuracy of the data analysis. All authors read and approved the final manuscript.

Data Availability Data available on request from the authors.

Declarations

Ethics approval This article is based on present cases and review of published literature, and complies with the Institutional Ethical Standards.

Conflict of interest The authors declare no competing interests.

References

1. Coffin CM FJ (2013) World Health Organization classification of tumors of soft tissue and bone. (ed 4), Lyon: IARC pp. 83
2. Collins K, Ramalingam P, Euscher ED et al (2021) Uterine inflammatory myofibroblastic neoplasms with aggressive behavior, including an epithelioid inflammatory myofibroblastic sarcoma: a clinicopathologic study of 9 cases. Am J Surg Pathol. https://doi.org/10.1097/PAS.0000000000001756
3. Bennett JA, Wang P, Wanjari P et al (2021) Uterine inflammatory myofibroblastic tumor: first report of a ROS1 fusion. Genes Chromosomes Cancer. https://doi.org/10.1002/gcc.22986
4. Haimes JD, Stewart CJR, Kudlow BA et al (2017) Uterine inflammatory myofibroblastic tumors frequently harbor ALK fusions with IGFBP5 and THBS1. Am J Surg Pathol 41:773–780. https://doi.org/10.1097/PAS.0000000000000801
5. Bennett JA, Nardi V, Rouzbahman M et al (2017) Inflammatory myofibroblastic tumor of the uterus: a clinicopathological, immunohistochemical, and molecular analysis of 13 cases highlighting their broad morphologic spectrum. Mod Pathol 30:1489–1503. https://doi.org/10.1038/modpathol.2017.69
6. Parra-Herran C, Quick CM, Howitt BE et al (2015) Inflammatory myofibroblastic tumor of the uterus: clinical and pathologic review of 10 cases including a subset with aggressive clinical course. Am J Surg Pathol 39:157–168. https://doi.org/10.1097/PAS.0000000000000330
7. Antonescu CR, Suurmeijer AJ, Zhang L et al (2015) Molecular characterization of inflammatory myofibroblastic tumors with frequent ALK and ROS1 gene fusions and rare novel RET rearrangement. Am J Surg Pathol 39:957–967. https://doi.org/10.1097/PAS.0000000000000404
8. Schoolmeester JK, Minn K, Sukov WR et al (2020) Uterine inflammatory myofibroblastic tumor involving the decidua of the extraplacental membranes: report of a case with a TIMP3-ROS1 gene fusion. Hum Pathol 100:45–46. https://doi.org/10.1016/j.humpath.2020.03.014
9. Cheek EH, Fadra N, Jackson RA et al (2020) Uterine inflammatory myofibroblastic tumors in pregnant women with and without involvement of the placenta: a study of 6 cases with identification of a novel TIMP3-RET fusion. Hum Pathol 97:29–39. https://doi.org/10.1016/j.humpath.2019.12.006
10. Takahashi A, Kurosawa M, Uemura M et al (2018) Anaplastic lymphoma kinase-negative uterine inflammatory myofibroblastic tumor containing the ETV6-NTRK3 fusion gene: a case report. J Int Med Res 46:3498–3503. https://doi.org/10.1177/0300060518780873
11. Zarei S, Abdul-Karim FW, Chase DM et al (2020) Uterine inflammatory myofibroblastic tumor showing an atypical ALK signal pattern by FISH and DES-ALK fusion by RNA sequencing: a case report. Int J Gynecol Pathol 39:152–156. https://doi.org/10.1097/PGP.0000000000000588
12. Makhdoum S, Nardi V, Devereaux KA et al (2020) Inflammatory myofibroblastic tumors associated with the placenta: a series of 9 cases. Hum Pathol 106:62–73. https://doi.org/10.1016/j.humpath.2020.09.005
13. Etlinger P, Kuthi L, Kovacs T (2020) Inflammatory myofibroblastic tumors in the uterus: childhood-case report and review of the literature. Front Pediatr 8:36. https://doi.org/10.3389/fped.2020.00036
14. Devereaux KA, Fitzpatrick MB, Hartinger S et al (2020) Pregnancy-associated inflammatory myofibroblastic tumors of the uterus are clinically distinct and highly enriched for TIMP3-ALK and THBS1-ALK fusions. Am J Surg Pathol 44:970–981. https://doi.org/10.1097/PAS.0000000000001481

15. Stikova Z, Ptakova N, Horakova M et al (2019) Inflammatory myofibroblastic tumor of the uterus - case report. Cesk Patol 55:239–243
16. Lee J, Singh A, Ali SM et al (2019) TNS1-ALK fusion in a recurrent, metastatic uterine mesenchymal tumor originally diagnosed as leiomyosarcoma. Acta Med Acad 48:116–120. https://doi.org/10.5644/ama2006-124.248
17. Squires L, Matsika A, Turner J et al (2018) ALK-rearranged inflammatory myofibroblastic tumour of placental membranes. Pathology 50:777–779. https://doi.org/10.1016/j.pathol.2018.05.008
18. Mohammad N, Haimes JD, Mishkin S et al (2018) ALK is a specific diagnostic marker for inflammatory myofibroblastic tumor of the uterus. Am J Surg Pathol 42:1353–1359. https://doi.org/10.1097/PAS.0000000000001120
19. Ladwig NR, Schoolmeester JK, Weil L et al (2018) Inflammatory myofibroblastic tumor associated with the placenta: short tandem repeat genotyping confirms uterine site of origin. Am J Surg Pathol 42:807–812. https://doi.org/10.1097/PAS.0000000000001044
20. Pickett JL, Chou A, Andrici JA et al (2017) Inflammatory myofibroblastic tumors of the female genital tract are under-recognized: a low threshold for ALK immunohistochemistry is required. Am J Surg Pathol 41:1433–1442. https://doi.org/10.1097/PAS.0000000000000909
21. Busca A, Parra-Herran C (2017) Myxoid mesenchymal tumors of the uterus: an update on classification, definitions, and differential diagnosis. Adv Anat Pathol 24:354–361. https://doi.org/10.1097/PAP.0000000000000164
22. Parra-Herran C, Schoolmeester JK, Yuan L et al (2016) Myxoid leiomyosarcoma of the uterus: a clinicopathologic analysis of 30 cases and review of the literature with reappraisal of its distinction from other uterine myxoid mesenchymal neoplasms. Am J Surg Pathol 40:285–301. https://doi.org/10.1097/PAS.0000000000000593
23. Subbiah V, McMahon C, Patel S et al (2015) STUMP un"stumped": anti-tumor response to anaplastic lymphoma kinase (ALK) inhibitor based targeted therapy in uterine inflammatory myofibroblastic tumor with myxoid features harboring DCTN1-ALK fusion. J Hematol Oncol 8:66. https://doi.org/10.1186/s13045-015-0160-2
24. Saeed H, Almardini N, Jacques SM et al (2015) Inflammatory myofibroblastic tumour: unexpected finding on placental examination. Eur J Obstet Gynecol Reprod Biol 194:254–255. https://doi.org/10.1016/j.ejogrb.2015.07.003
25. Fraggetta F, Doglioni C, Scollo P et al (2015) Uterine inflammatory myofibroblastic tumor in a 10-year-old girl presenting as polypoid mass. J Clin Oncol 33:e7–e10. https://doi.org/10.1200/JCO.2013.48.8304
26. Banet N, Ning Y, Montgomery EA (2015) Inflammatory myofibroblastic tumor of the placenta: a report of a novel lesion in 2 patients. Int J Gynecol Pathol 34:419–423. https://doi.org/10.1097/PGP.0000000000000175
27. Kushnir CL, Gerardi M, Banet N et al (2013) Extrauterine inflammatory myofibroblastic tumor: a case report. Gynecol Oncol Case Rep 6:39–41. https://doi.org/10.1016/j.gynor.2013.07.007
28. Fuehrer NE, Keeney GL, Ketterling RP et al (2012) ALK-1 protein expression and ALK gene rearrangements aid in the diagnosis of inflammatory myofibroblastic tumors of the female genital tract. Arch Pathol Lab Med 136:623–626. https://doi.org/10.5858/arpa.2011-0341-OA
29. Olgan S, Saatli B, Okyay RE et al (2011) Hysteroscopic excision of inflammatory myofibroblastic tumor of the uterus: a case report and brief review. Eur J Obstet Gynecol Reprod Biol 157:234–236. https://doi.org/10.1016/j.ejogrb.2011.02.016
30. Gupta N, Mittal S, Misra R (2011) Inflammatory pseudotumor of uterus: an unusual pelvic mass. Eur J Obstet Gynecol Reprod Biol 156:118–119. https://doi.org/10.1016/j.ejogrb.2011.01.002
31. Shintaku M, Fukushima A (2006) Inflammatory myofibroblastic tumor of the uterus with prominent myxoid change. Pathol Int 56:625–628. https://doi.org/10.1111/j.1440-1827.2006.02018.x
32. Rabban JT, Zaloudek CJ, Shekitka KM et al (2005) Inflammatory myofibroblastic tumor of the uterus: a clinicopathologic study of 6 cases emphasizing distinction from aggressive mesenchymal tumors. Am J Surg Pathol 29:1348–1355. https://doi.org/10.1097/01.pas.0000172189.02424.91
33. Gucer F, Altaner S, Mulayim N et al (2005) Invasive inflammatory pseudotumor of uterine cervix: a case report. Gynecol Oncol 98:325–328. https://doi.org/10.1016/j.ygyno.2005.05.021
34. Dehner LP (2004) Inflammatory myofibroblastic tumor: the continued definition of one type of so-called inflammatory pseudotumor. Am J Surg Pathol 28:1652–1654. https://doi.org/10.1097/00000478-200412000-00016
35. Azuno Y, Yaga K, Suehiro Y et al (2003) Inflammatory myoblastic tumor of the uterus and interleukin-6. Am J Obstet Gynecol 189:890–891. https://doi.org/10.1067/s0002-9378(03)00208-4
36. Kargi HA, Ozer E, Gokden N (1995) Inflammatory pseudotumor of the uterus: a case report. Tumori 81:454–456
37. Abenoza P, Shek YH, Perrone T (1994) Inflammatory pseudotumor of the cervix. Int J Gynecol Pathol 13:80–86. https://doi.org/10.1097/00004347-199401000-00010
38. Gilks CB, Taylor GP, Clement PB (1987) Inflammatory pseudotumor of the uterus. Int J Gynecol Pathol 6:275–286. https://doi.org/10.1097/00004347-198709000-00008
39. Kuisma H, Jokinen V, Pasanen A et al (2022) Histopathologic and molecular characterization of uterine leiomyoma-like inflammatory myofibroblastic tumor: comparison to molecular subtypes of uterine leiomyoma. Am J Surg Pathol 46:1126–1136. https://doi.org/10.1097/PAS.0000000000001904
40. Li Z, Shen L, Ding D et al (2018) Efficacy of crizotinib among different types of ROS1 fusion partners in patients with ROS1-rearranged non-small cell lung cancer. J Thorac Oncol 13:987–995. https://doi.org/10.1016/j.jtho.2018.04.016
41. Iyer SR, Odintsov I, Schoenfeld AJ et al (2022) MYC promotes tyrosine kinase inhibitor resistance in ROS1-fusion-positive lung cancer. Mol Cancer Res 20:722–734. https://doi.org/10.1158/1541-7786.MCR-22-0025
42. Dietz S, Christopoulos P, Gu L et al (2019) Serial liquid biopsies for detection of treatment failure and profiling of resistance mechanisms in KLC1-ALK-rearranged lung cancer. Cold Spring Harb Mol Case Stud 5(6):a004630. https://doi.org/10.1101/mcs.a004630
43. Lee CJ, Schoffski P, Modave E et al (2021) Comprehensive molecular analysis of inflammatory myofibroblastic tumors reveals diverse genomic landscape and potential predictive markers for response to crizotinib. Clin Cancer Res 27:6737–6748. https://doi.org/10.1158/1078-0432.CCR-21-1165